Hindawi
Journal of Nanomaterials
Volume 2017, Article ID 2560436, 6 pages
https://doi.org/10.1155/2017/2560436

Research Article

Effect of Annealing Temperature and Spin Coating Speed on Mn-Doped ZnS Nanocrystals Thin Film by Spin Coating

Noor Azie Azura Mohd Arif,[1] Chong Chee Jiun,[1] and Sahbudin Shaari[2]

[1]*Centre for Pre-University Studies, Universiti Malaysia Sarawak, 94300 Kota Samarahan, Sarawak, Malaysia*
[2]*Institute of Microengineering and Nanoelectronics, Universiti Kebangsaan Malaysia, 43600 Bangi, Selangor, Malaysia*

Correspondence should be addressed to Noor Azie Azura Mohd Arif; manaazura@unimas.my

Received 7 October 2016; Revised 13 December 2016; Accepted 19 December 2016; Published 4 January 2017

Academic Editor: Biswanath Bhoi

ZnS:Mn nanocrystals thin film was fabricated at 300°C and 500°C via the spin coating method. Its sol-gel was spin coated for 20 s at 3000 rpm and 4000 rpm with metal tape being used to mold the shape of the thin film. A different combination of these parameters was used to investigate their influences on the fabrication of the film. Optical and structural characterizations have been performed. Optical characterization was analyzed using UV-visible spectroscopy and photoluminescence spectrophotometer while the structural and compositional analysis of films was measured via field emission scanning electron microscopy and energy dispersive X-ray. From UV-vis spectra, the wavelength of the ZnS:Mn was 250 nm and the band gap was within the range 4.43 eV–4.60 eV. In room temperature PL spectra, there were two emission peaks centered at 460 nm and 590 nm. Under higher annealing temperature and higher speed used in spin coating, an increase of 0.05 eV was observed. It was concluded that the spin coating process is able to synthesize high quality spherical ZnS:Mn nanocrystals. This conventional process can replace other high technology methods due to its synthesis cost.

1. Introduction

ZnS is one of the most studied nanomaterials. It is relatively easy to fabricate the nanomaterial with the intended optical and electrical properties through controlling the shape of its nanostructure [1, 2]. It has a wide energy band gap with a value of 3.68 eV for cubic phase and 3.77 eV for hexagonal phase [3–10]. There are several physical methods (ion sputtering, laser ablation, gas condensation, pyrolysis, etc.) and chemical methods (solvothermal, photochemical, electrochemical, thermolytic, sol-gel, etc.) to synthesize nanocrystalline thin film and to control its crystal size [11]. Sol-gel is a cheap chemical method that fabricates material through the process of phase change from liquid phase (sol) to solid phase (gel) [12–14]. Fabrication that employs this method will usually be entailed by either spin coating or dip coating process followed by heat treatment process. Walker et al. (1995) found that annealing treatment is required to reduce material defects. Annealing treatment is a common procedure in fabrication of nanomaterial to either improve the quality of crystal or stabilize the structure at a temperature [15]. Due to the fact that the dopant is able to extend the capability of a semiconductor compound, this work focused on doped ZnS. Besides, the luminance color of the doped material changes according to the dopant used. The commonly used dopant is manganese ions (Mn^{2+}) and copper ions (Cu^{2+}). Mn^{2+} produces orange emission while Cu^{2+} produces green emission [16–19]. Parameters such as annealing temperature and speed of rotation were used in these experiments to investigate their influence on the fabrication of nanocrystalline thin film. Based on [20–22], the influence of the spin coating speed will affect the band gap of the thin film. The band gap increases roughly with the increase in annealing temperature and spin coating speed. This work aims to identify the characteristics of zinc sulphide doped manganese (ZnS:Mn) fabricated using several combinations of annealing temperatures and speeds of spin coating.

2. Methodology

In this study, ZnS:Mn thin films were prepared using the conventional triple process (sol-gel, self-assembly, and spin coating process). The morphology and composition of the films were studied using a field emission scanning electron microscope (FE-SEM) (model Zeiss Supra 55) and energy dispersive X-ray (EDX) while the optical properties of the film were studied using a photoluminescence (PL) spectrometer (model Perkin Elmer LS 55) and ultraviolet-visible spectroscopy (UV-Vis) (model Lambda 650, Perkin Elmer). Characterization was done at room temperature. Sections 2.1 and 2.2 describe each fabrication step in detail.

2.1. Preparation of Sol. The solution was prepared according to the formula $Zn_{(1-x)}Mn_xS$ at $x = 0.05$ using hydrated zinc nitrate, manganese acetate, thiourea, 2-propanol, hydrochloric acid, and distilled water. In the reaction, hydrated zinc nitrate and manganese acetate were dissolved in 2-propanol and distilled water to produce zinc and manganese ions. Then, hydrochloric acid was added to the solution as a catalyst. After 5 seconds, thiourea was added to the solution to produce sulfur. A clear solution was produced after 48 hours of stirring. Equations (1)–(3) describe the reactions that took place during the preparation while (4) describes the overall preparation process.

$$\mathrm{Zn(NO_3)_2 \cdot 6H_2O \longrightarrow Zn^{2+} + 2(NO_3)^- + 6H_2O} \quad (1)$$

$$\mathrm{Mn(CH_3COO)_2 \cdot 2H_2O \longrightarrow Mn^{2+} + 2(CH_3COO)^- + 2H_2O} \quad (2)$$

$$\mathrm{NH_2CSNH_2 + 2H_2O \longrightarrow H_2S + CH_3COO^- + NH_4^+} \quad (3)$$

$$\mathrm{Zn(NO_3)_2 \cdot 6H_2O + Mn(CH_3COO)_2 \cdot 2H_2O + H_2S \longrightarrow ZnS : (Mn^{+2}) + 2H^+ + 2(NO_3)^- + 8H_2O + 2(CH_3COO)^-} \quad (4)$$

2.2. Preparation of Thin Film. ZnS:Mn sol was deposited on a glass substrate using a spin coater (model WS-400BX-6NPP/LITE). The sample was rotated with high efficiency at the speed of 3000 rpm for 20 seconds. During the process, the centripetal acceleration spread the sol in all directions and the thin film could only be produced by sol that adhered on the surface of the substrate. In order to maximize the amount of sol that could adhere on the substrate, a metal tape was placed on the substrate acting as a wall to hold the structure of the sol during the spin coating process. This process was repeated with another spin coating speed of 4000 rpm to observe the effect of speed on the material produced. During the deposition process, the arrangement of the particles in nanocrystalline ZnS:Mn remained unorganized. Heat treatment was used to reduce material defects. After that, the thin film was cooled to room temperature at normal rates. Figure 1 shows the position of glass substrate during the heating process. Two heating temperatures (300°C and 500°C) were used to study the influence of heat temperature on the optical and microstructural properties of the thin films produced.

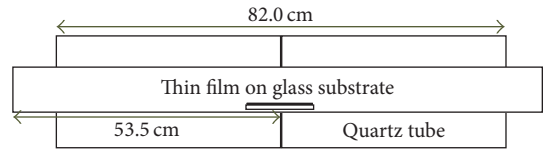

Figure 1: Position of the substrate during the annealing process.

3. Results and Discussion

3.1. Photoluminescent (PL) Spectra. Figures 2(a) and 2(b) display the spectrum of photoluminescence for all the thin films when they underwent the 250 nm excitation wavelength. In both figures, three emission spectra were observed. The first peak was produced within wavelength ranging from 350 to 450 nm. This is evident to the recombination of electron trapped in the energy gap of ZnS [23]. From an earlier research investigation, it was mentioned that the emission was not affected by the Mn dopant [24, 25]. The second peak is the highest located at the center (500 nm) and was generated due to the impact of the first excited wavelength of 250 nm. This huge peak at 500 nm is not related to the sample. Lastly, the orange emission peak at 590 nm was attributed to $^4T_1 \rightarrow {}^6A_1$ transition in d-orbital of Mn^{2+}. Besides these three bands, a small peak can be observed at 460 nm which was caused by the presence of Mn ions (d-orbital) in the host lattice ZnS [26].

3.2. Absorption and Transmittance Spectra. It is well known that the effect of 3D quantum confinement only occurs when the size of nanocrystals is equal to de Broglie wavelength of electrons or holes. The resulting shift in the semiconductor absorption is a consequence of quantum confinement related to the improvement of energy gap between valence and conduction band. Figures 3(a) and 3(b) show the absorption spectrum for thin films produced at different speeds of spin coating and temperatures of annealing treatment. In these figures, the absorption peak occurred at around 250 nm. The resulting spectrum was a blue shift which was different with the bulk ZnS (345 nm). Based on previous studies, ZnS has great potential to absorb light at wavelength ranging between 220 nm and 350 nm [4].

Transmittance spectra, which are the inverse in the absorption spectrum, showed that almost 85% transmittance is within the visible range. As shown in Figures 4(a) and 4(b), the sharp fall of transmittance spectrum occurs in the vicinity of energy band region. The absorption coefficient α can be calculated from the data of transmittance using Manifacier model [27].

3.3. Optical Energy Band Gap E_g. The energy band gap E_g for the thin films was studied as well. These values were obtained from the plot of $(\alpha h\nu)^2$ against $h\nu$ by superimposing a straight line on the data points as shown in Figure 5. The values of

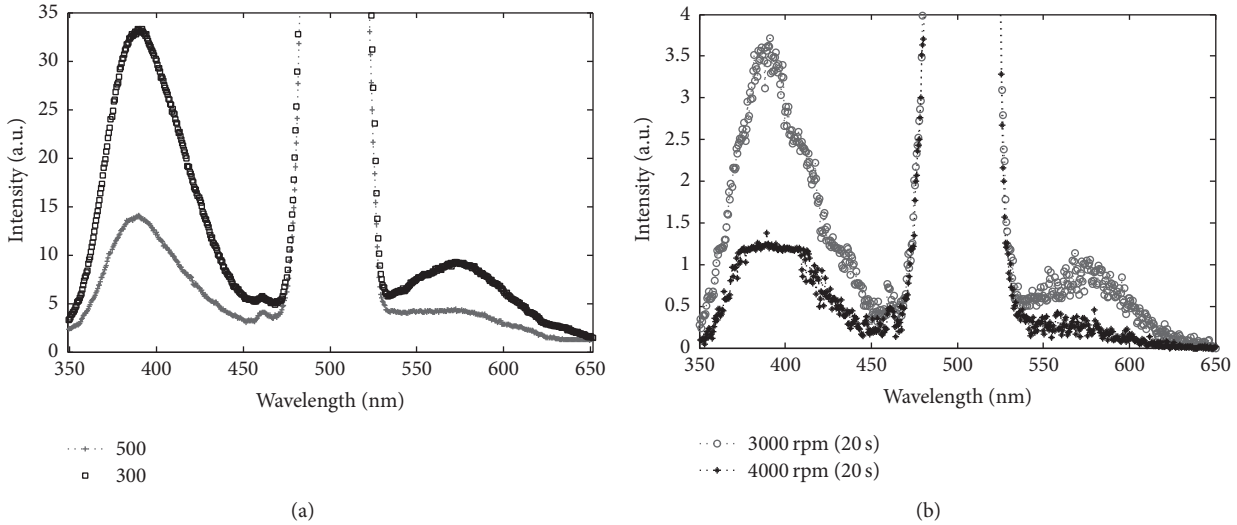

Figure 2: Photoluminescence spectra of Mn-doped ZnS nanocrystals at different (a) temperatures and (b) times and speeds of rotation.

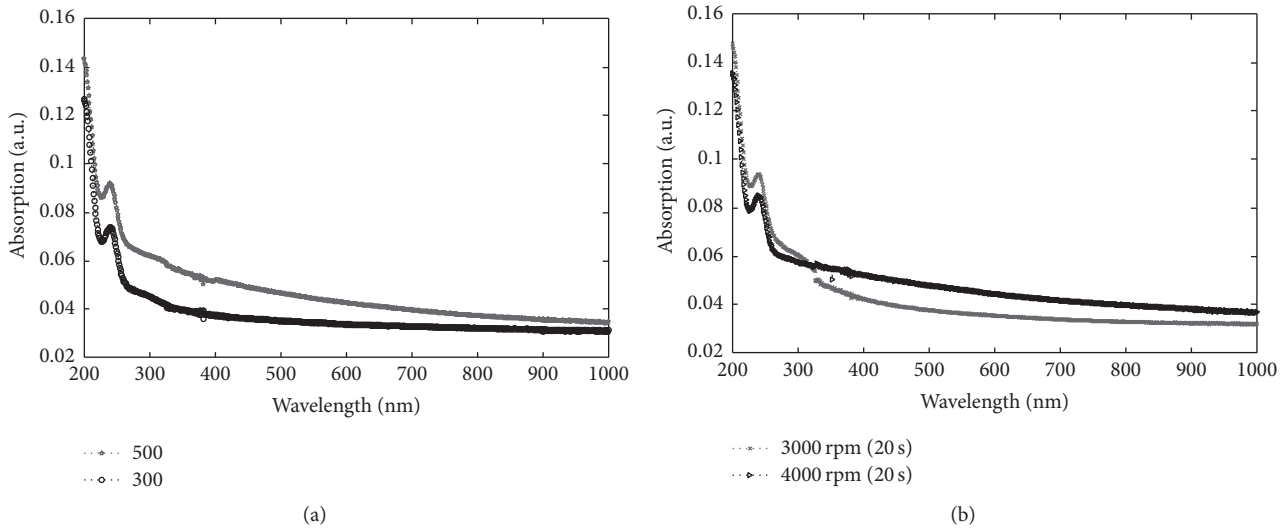

Figure 3: The absorption spectra of ZnS:Mn nanocrystals fabricated at different (a) temperatures and (b) times and speeds of rotation.

E_g obtained were around 4.43 eV–4.60 eV depending on the fabrication procedure chosen.

3.4. Effect of Annealing Temperature. Figure 2(a) shows that the intensity of the emission spectrum decreases with an increase in annealing temperature. The level of intensity dropped from 41 a.u. to 14 a.u. for the first emission band while the level for the last emission dropped from 13 a.u. to 4 a.u. for the third emission. Even the small peak at 460 nm dropped as well but it was not as much as the other two emission bands. The higher temperature caused more Mn^{2+} ions to be released from the ZnS matrix which lowered the peak at 590 nm. Besides degradation in the intensity spectrum, higher annealing temperature also increases the light absorption ability of the thin film. From Figure 3(a), the low annealing treatment dampens the absorption ability in the visible region. For transmittance level shown in Figure 4(a), the sharp fall region for both thin films is within the same range regardless of the annealing temperature used. The level of transmittance in visible range remained at an equal level as well.

In the study of energy band gap, the thin film that was produced under higher annealing temperature has higher E_g value of 4.60 eV. But the increase was only at 0.05 eV. The increase in the energy band gap, absorption, and intensity spectrum could be attributed to the reduction in the size of particles adhered on the substrate as shown in Figure 6. From the FE-SEM images, the size of the spherical particles produced under annealing temperatures 300°C and 500°C was 30.0–36.8 nm and 21.8–23.2 nm, respectively. These images prove that the size of particles reduced when the annealing temperature was raised. This occurred because of potential and kinetic energy during the annealing process [28]. Figure 7 shows the EDX result of ZnS:Mn thin film with composition

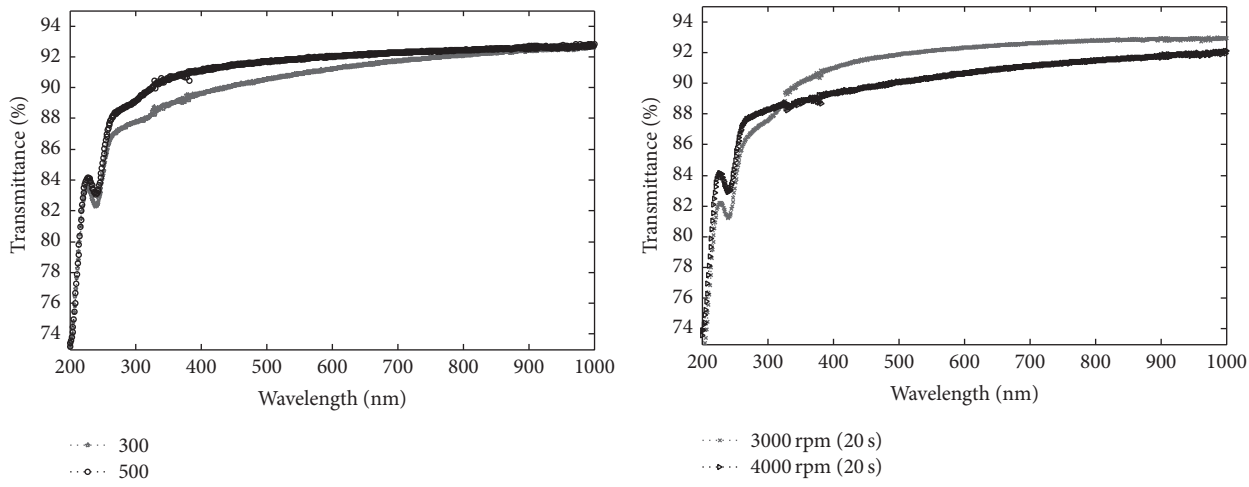

Figure 4: Transmittance spectra of ZnS:Mn nanocrystals fabricated at different (a) temperatures and (b) times and speeds of rotation.

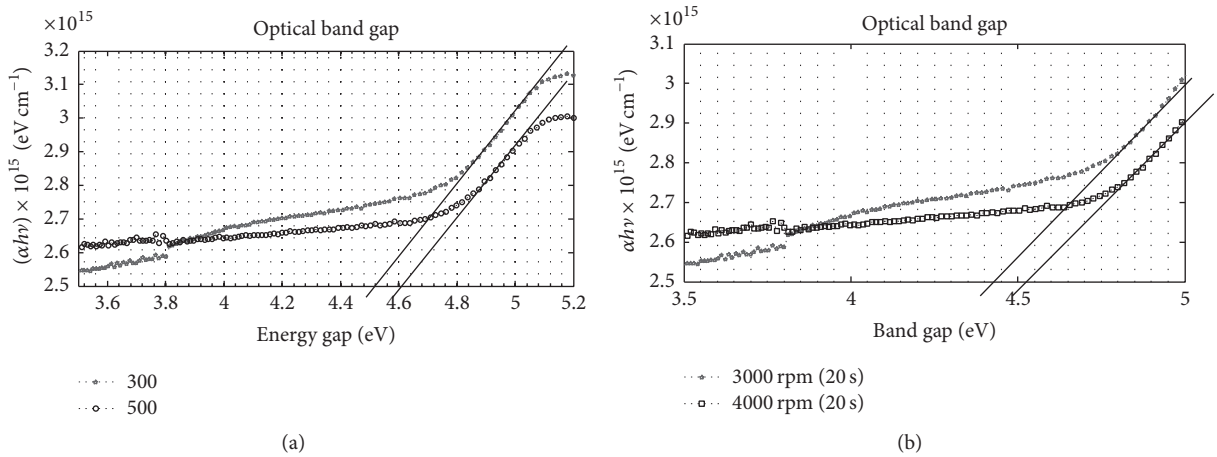

Figure 5: Measurement of the energy gap of ZnS:Mn nanocrystals fabricated at different (a) temperatures and (b) times and speeds of rotation.

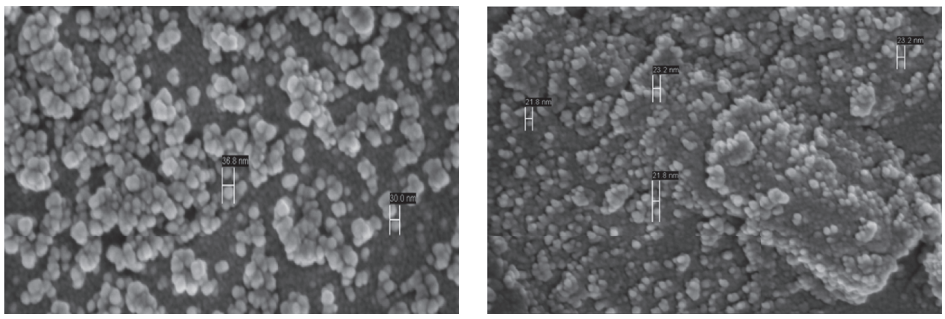

Figure 6: Nanocrystalline thin film produced at the heating temperatures of (a) 300°C and (b) 500°C with grain sizes of 30.0–36.8 nm and 21.8–23.2 nm, respectively.

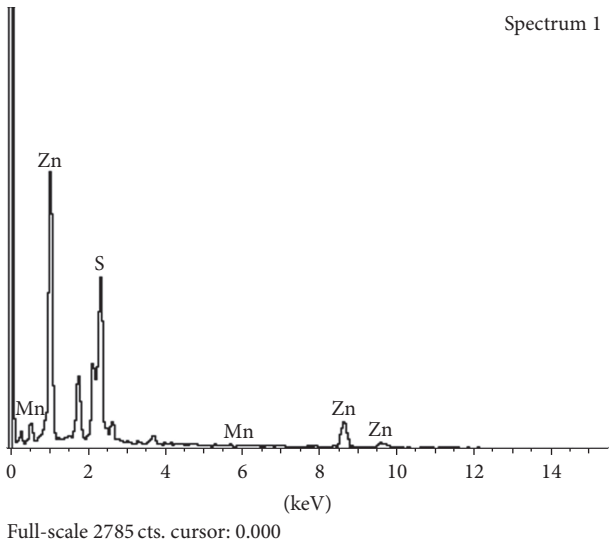

Figure 7: EDX result of ZnS:Mn thin film with composition $Zn_{(1-x)}Mn_xS$ at $x = 0.05$.

$Zn_{(1-x)}Mn_xS$ at $x = 0.05$. The proportion of the constituent elements measured was Zn = 65.33%, S = 26.84%, and Mn = 7.83%.

3.5. Effect of Spin Coating Speed. From Figure 2(b), a decrease in the intensity of the emission spectrum for the first and third band is observed when a higher speed of spin coating was used in the deposition process. The intensity of the thin film that underwent higher speed of coating dropped by at least 50% compared to the intensity emitted by another thin film. For the first band, the peak dropped drastically from 3.8 a.u. to 1.3 a.u. while a smaller drop occurred at the third band from 1.1 a.u. to 0.5 a.u. These drops suggest that a slower speed of spin coating should be chosen if high level of intensity in the emission of thin film is a desired property.

From the absorption spectra in Figure 3(b), the light absorption ability in the thin film that underwent higher speed of spin coating is weaker but the differences are not as obvious as the differences observed in the emission spectra. In terms of transmittance, the sharp fall region for both thin films is within the same range again as shown in Figure 4(b). However, for the thin film that underwent higher speed of spin coating, the transmittance level was slightly higher but still within the visible range. For the study of energy band gap, E_g value is found to be higher for the thin film that was fabricated using higher speed of spin coating. When produced at 4000 rpm, the energy band gap was found to be 4.53 eV while it was 4.43 eV for another thin film. This suggests that the nanoparticles of the thin film produced via higher speed of spin coating were smaller. The reduction of particle size as well as thin film thickness can be verified using general relationship (5) [29, 30]. Generally, by calculating or plotting using the experimental values $w = 3000$ rpm (20 s) and $w = 4000$ rpm (20 s), the relation between thickness H and spin rotation can be determined:

$$H \propto w^{-1} t^{-0.5}. \quad (5)$$

4. Conclusions

Spherical ZnS:Mn nanocrystals thin films with grain size of 21.8–36.8 nm have been fabricated via spin coating method with thin film being molded by a metal tape at the spin coating stage. The UV-vis spectra of the ZnS:Mn nanocrystals reveal that the limiting wavelength is 250 nm. The PL spectra for different temperatures show that the decrement in annealing temperature increases the maximum properties. The PL spectra display blue and orange emission while the absorption edge appears at around 250 nm. From the measurements of transmittance for the films, the direct band gap values have been measured and they fall within the range 4.43 eV–4.60 eV. This conventional process is a simple and very useful method to synthesize high quality sphere-like ZnS:Mn nanocrystals thin films. It will be a promising low-*cost* alternative to other high technology methods in the future.

Competing Interests

The authors declare that they have no competing interests.

Acknowledgments

This work was supported by Universiti Kebangsaan Malaysia Research University Grant and Universiti Malaysia Sarawak Research University Grant (RAGS/SG01(1)/1310/2015(04)), which is gratefully acknowledged.

References

[1] S. Hamad, S. M. Woodley, and C. R. A. Catlow, "Experimental and computational studies of ZnS nanostructures," *Molecular Simulation*, vol. 35, no. 12-13, pp. 1015–1032, 2009.

[2] S. Nadana, C. Shanmugam, S. Arumugam, V. Govindan, and K. Nadesan, "Temperature controlled synthesis of ZnS nanocrystals by simple chemical precipitation," *Walailak Journal of Science and Technology*, vol. 10, no. 2, pp. 149–157, 2013.

[3] K. Manzoor, V. Aditya, S. R. Vadera, N. Kumar, and T. R. N. Kutty, "Spontaneous organisation of ZnS nanoparticles into monocrystalline nanorods with highly enhanced dopant-related emission," *Journal of Physics and Chemistry of Solids*, vol. 66, no. 7, pp. 1164–1170, 2005.

[4] L. W. Schwartz, "Analysis of spin coating for non-ideal conditions," in *Proceedings of the International Coating Science and Technology Symposium*, 2008.

[5] P. M. B. Walker, *The Wordsworth Dictionary of Science & Technology*, Wordsworth Editions, Hertfordshire, UK, 1995.

[6] K. H. Yoon, J. K. Ahn, and J. Y. Cho, "Optical characteristics of undoped and Mn doped ZnS films," *Journal of Materials Science*, vol. 36, no. 6, pp. 1373–1376, 2001.

[7] T. M. Thi, N. T. Hien, D. X. Thu, and V. Q. Trung, "Thin films containing Mn-doped ZnS nanocrystals synthesised by chemical method and study of some of their optical properties," *Journal of Experimental Nanoscience*, vol. 8, no. 5, pp. 530–538, 2013.

[8] F. A. La Porta, J. Andrés, M. S. Li, J. R. Sambrano, J. A. Varela, and E. Longo, "Zinc blende versus wurtzite ZnS nanoparticles: control of the phase and optical properties by tetrabutylammonium hydroxide," *Physical Chemistry Chemical Physics*, vol. 16, no. 37, pp. 20127–20137, 2014.

[9] H. A. T. Al-Ogaili, "Synthesis of colloidal zinc sulfide nanoparticle via chemical route and its structural and optical properties," *International Journal of Advanced Research in Science, Engineering and Technology*, vol. 3, no. 3, pp. 1587–1592, 2016.

[10] F. Al-Sagheer, A. Bumajdad, M. Madkour, and B. Ghazal, "Optoelectronic characteristics of ZnS quantum dots: Simulation and experimental investigations," *Science of Advanced Materials*, vol. 7, no. 11, pp. 2352–2360, 2015.

[11] F. M. Daniel, *Novel ZnS nanostructures: synthesis, growth, mechanism and applications [Ph.D. thesis]*, Georgia Institute of Technology, 2006.

[12] A. A. M. A. Noor, S. Shaari, and S. A. R. Mohammad, "Improving the production of self-assembled ZnS:Mn nanocrystals through the modification of sol gel—spin coating approaches," *Advanced Materials Research*, vol. 1024, pp. 23–26, 2014.

[13] Q. Ma, Q. Xu, C.-L. Tsai, F. Tietz, and O. Guillon, "A novel sol-gel method for large-scale production of nanopowders: preparation of $Li_{1.5}Al_{0.5}Ti_{1.5}(PO_4)_3$ as an example," *Journal of the American Ceramic Society*, vol. 99, no. 2, pp. 410–414, 2016.

[14] G. J. Owens, R. K. Singh, F. Foroutan et al., "Sol-gel based materials for biomedical applications," *Progress in Materials Science*, vol. 77, pp. 1–79, 2016.

[15] N. Shanmugam, S. Cholan, N. Kannadasan, K. Sathishkumar, and G. Viruthagiri, "Effect of annealing on the zns nanocrystals prepared by chemical precipitation method," *Journal of Nanomaterials*, vol. 2013, Article ID 351798, 7 pages, 2013.

[16] N. Onuma, *Synthesis and characterization of nanocrystalline ZnS:Mn^{2+} polyelectrolyte [Tesis Sarjana]*, Mahidol University, 2005.

[17] S. Prabha, H. Lubna, and M. M. Malik, "Luminescence and morphological kinetics of functionalized ZnS colloidal nanocrystals," *ISRN Optics*, vol. 2012, Article ID 621908, 8 pages, 2012.

[18] Z. Paulina, M. Ewa, and P. Malgorzata, "ZnS Cu-doped quantum dots," *Biotechnology and Food Sciences*, vol. 78, no. 1, pp. 53–69, 2014.

[19] S. Pramanik, S. Bhandari, S. Roy, and A. Chattopadhyay, "Synchronous tricolor emission-based white light from quantum dot complex," *The Journal of Physical Chemistry Letters*, vol. 6, no. 7, pp. 1270–1274, 2015.

[20] A. A. David, M. A. Saint, and A. Oluwaseun, "Effect of spin coating speed on some optical properties of ZnO thin films," *Journal of Materials Science and Chemical Engineering*, vol. 4, pp. 1–6, 2016.

[21] A. Battal, D. Tatar, A. Kocyigit, and B. Duzgun, "Comparison effect of spin speeds and substrate layers on properties of doubly doped tin oxide thin films prepared by SOL-GEL spin coating method," *Journal of Ovonic Research*, vol. 10, no. 2, pp. 23–34, 2014.

[22] T. D. Malevu and R. O. Ocaya, "Effect of annealing temperature on structural, morphology and optical properties of ZnO nanoneedles prepared by Zinc-Air system method," *International Journal of Electrochemical Science*, vol. 10, pp. 1752–1761, 2015.

[23] E. Mohagheghpour, M. Rabiee, F. Moztarzadeh et al., "Controllable synthesis, characterization and optical properties of ZnS:Mn nanoparticles as a novel biosensor," *Materials Science and Engineering C*, vol. 29, no. 6, pp. 1842–1848, 2009.

[24] W. Q. Peng, S. C. Qu, G. W. Cong, X. Q. Zhang, and Z. G. Wang, "Optical and magnetic properties of ZnS nanoparticles doped with Mn^{2+}," *Journal of Crystal Growth*, vol. 282, no. 1-2, pp. 179–185, 2005.

[25] W. Q. Peng, S. C. Qu, G. W. Cong, and Z. G. Wang, "Concentration effect of Mn^{2+} on the photoluminescence of ZnS:Mn nanocrystals," *Journal of Crystal Growth*, vol. 279, no. 3-4, pp. 454–460, 2005.

[26] D. Mohanta, G. A. Ahmed, A. Choudhury, F. Singh, and D. K. Avasthi, "Properties of 80-MeV oxygen ion irradiated ZnS:Mn nanoparticles and exploitation in nanophotonics," *Journal of Nanoparticle Research*, vol. 8, no. 5, pp. 645–652, 2006.

[27] R. Maity and K. K. Chattopadhyay, "Synthesis and optical characterization of ZnS and ZnS:Mn nanocrystalline thin films by chemical route," *Nanotechnology*, vol. 15, no. 7, pp. 812–816, 2004.

[28] M. S. Ab-Rahman, N. A. A. M. Arif, and S. Shaari, "Effect of thermal treatment on the morphology of ZnS: Mn nanocrystals," *World Applied Sciences Journal*, vol. 12, no. 9, pp. 1505–1511, 2011.

[29] E. Mohajerani, F. Farajollahi, R. Mahzoon, and S. Baghery, "Morphological and thickness analysis for PMMA spin coated films," *Journal of Optoelectronics and Advanced Materials*, vol. 9, no. 12, pp. 3901–3906, 2007.

[30] V. Stanić, T. H. Etsell, A. C. Pierre, and R. J. Mikula, "Sol-gel processing of ZnS," *Materials Letters*, vol. 31, no. 1-2, pp. 35–38, 1997.